Heliyon 10 (2024) e34600

Contents lists available at ScienceDirect

Heliyon

journal homepage: www.cell.com/heliyon

Research article

Novel analysis of functional relationship linking moyamoya disease to moyamoya syndrome

Lei Cao [a], Wenzhi Yang [b], Xiaozong Duan [a], Yipu Shao [a], Zhizhong Zhang [a], Chenchao Wang [a], Kaiwen Sun [a], Manxia Zhang [a], Hongwei Li [a,**], Kouji H. Harada [c,***], Bo Yang [a,*]

[a] Department of Neurosurgery, The First Affiliated Hospital of Zhengzhou University, Zhengzhou, 450000, China
[b] School of Life Science, Zhengzhou University, Zhengzhou, 450000, China
[c] Department of Health and Environmental Sciences, Kyoto University Graduate School of Medicine, Kyoto, 6068501, Japan

ARTICLE INFO

Keywords:
Moyamoya disease
Moyamoya syndrome
Genetic pathology
Bioinformatics analysis
KEGG
GO term
Protein-protein interaction

ABSTRACT

Objective: The aim of this study was to elucidate the genetic pathways associated with Moyamoya disease (MMD) and Moyamoya syndrome (MMS), compare the functional activities, and validate relevant related genes in an independent dataset.
Methods: We conducted a comprehensive search for genetic studies on MMD and MMS across multiple databases and identified related genes. Gene Ontology (GO) and Kyoto Encyclopedia of Genes and Genomes (KEGG) pathway enrichments analyses were performed for these genes. Commonly shared genes were selected for further validation in the independent dataset, GSE189993. The Sangerbox platform was used to perform statistical analysis and visualize the results. $P < 0.05$ indicated a statistically significant result.
Results: We included 52 MMD and 51 MMS-related publications and identified 126 and 51 relevant genes, respectively. GO analysis for MMD showed significant enrichment in cytokine activity, cell membrane receptors, enzyme binding, and immune activity. A broader range of terms was enriched for MMS. KEGG pathway analysis for MMD highlighted immune and cellular activities and pathways related to MMS prominently featured inflammation and metabolic disorders. Notably, nine overlapping genes were identified and validated. The expressions of RNF213, PTPN11, and MTHFR demonstrated significant differences in GSE189993. A combined receiver operating characteristic curve showed high diagnostic accuracy (AUC = 0.918).
Conclusions: The findings indicate a close relationship of MMD with immune activity and MMS with inflammation, metabolic processes and other environmental factors in a given genetic background. Differentiating between MMD and MMS can enhance the understanding of their pathophysiology and inform the strategies for their diagnoses and treatment.

* Corresponding author. No.1 Jianshe East Road, Erqi District, Zhengzhou City, Henan Province, China, 450000.
** Corresponding author. No.1 Jianshe East Road, Erqi District, Zhengzhou City, Henan Province, China, 450000.
*** Corresponding author. Yoshida Konoe, Sakyo, Kyoto, Japan, 6068501.
E-mail addresses: hongwei706@126.com (H. Li), kharada-hes@umin.ac.jp (K.H. Harada), yangbo96@163.com (B. Yang).

https://doi.org/10.1016/j.heliyon.2024.e34600
Received 16 February 2024; Received in revised form 10 July 2024; Accepted 12 July 2024
Available online 18 July 2024

Abbreviations

MMD	Moyamoya disease
MMS	Moyamoya syndrome
MMV	Moyamoya vasculopathy
MMA	Moyamoya arteriopathy
ICA	Internal carotid artery
SNP	Single-nucleotide polymorphisms
DSA	Digital subtraction angiography
PPI	Protein–protein interactions
GO	Gene Ontology
KEGG	Kyoto Encyclopedia of Genes and Genomes
BP	Biological process
CC	Cellular component
MF	Molecular function
MCA	Middle cerebral artery
ROC	Receiver operating characteristic

1. Introduction

Moyamoya disease (MMD), a rare cerebrovascular disease, is characterized by progressive spontaneous bilateral occlusion of the intracranial internal cerebral arteries (ICA) and their major branches with compensatory capillary collaterals resembling a "puff of smoke" [1]. Likewise, moyamoya syndrome (MMS) corresponds to a typical moyamoya angiopathy accompanied by another underlying condition quasi-moyamoya disease. According to the definition, the pathologic cerebral arteries are bilateral in MMD [1]. Cerebral angiography with unilateral findings suggests MMS, even if no other associated risk factors are present [2]. However, contralateral disease eventually develops in up to 40 % of patients who initially present with unilateral findings [3]. Altered vessels in pathological angiopathy are referred to as moyamoya vasculopathy (MMV) or moyamoya arteriopathy (MMA). Though clinical presentation [4], imaging features [5] and surgical management [6,7] of MMD and MMS have been reviewed previously, few studies have extensively compared and distinguished the relationship between MMD and MMS in biological processes. MMD and MMS could be triggered by different reasons but present the same imaging features. They may share common pathways in pathological development. It is crucial to differentiate MMD from MMS at the genetic and functional levels to advance the comparative study of MMD and MMS in the field of pathogenesis. Therefore, understanding the functional differences between MMD and MMS is critical to achieving potential far-reaching clinical implications in the future, including revealing pathological mechanisms, obtaining more accurate diagnostic markers, and developing clinical treatment strategies.

Though MMD has been reported worldwide, its pathophysiology remains unknown. Genetic factors are likely to play an essential role in moyamoya. There is a higher incidence of MMD in East Asia, especially Japan, Korea, and China, than in Europe, America, Africa, and Latin America [8]. The proportion of affected first-degree relatives reaches up to 15 % in Japan, and a corresponding rate of 6 % has been reported in the United States [9]. Familial cases are rare and limited to few reports in Caucasians [10]. The lower familial occurrence may account for the higher influence of genetic factors in Asian populations [11]. Over the last decades in genetic research, genetic linkage studies, association studies, and DNA sequencing techniques have been rapidly developed and applied. Linkage analyses have demonstrated five loci linked to MMD: 3p24.2-p26 [12], 6q25 [13], 8q23 [14], 12p12 [14], and 17q25 [15]. Association studies have revealed the association between single-nucleotide polymorphisms (SNPs) and MMD. Sequencing techniques have also revealed several potential candidate genes. These findings have contributed to a better understanding of the pathophysiological mechanism underlying MMD. Previous studies have identified genetic markers for MMD and MMS, such as *RNF213* [16,17], however, the functional activities linking these diseases remain poorly understood.

In the study, we aimed to uncover the similarities and differences in signaling pathways between MMD and MMS. Specifically, we attempted to: a) identify the genetic pathways involved in MMD and MMS; b) evaluate the functional similarities between MMD and MMS, and c) validate these identified genes in an independent dataset. This study is the first to compare functional activities based on genetic network analysis. We employed a novel approach by analyzing previously published susceptibility-related genes identified by bioinformatics analysis.

2. Methods and materials

2.1. Data collection

Articles for this study were screened by searching databases until March 2023, including PubMed, Web of Science and Google Scholar. No filters were applied during the search process. For Moyamoya disease, the following key terms were used: “Moyamoya disease”, “RNF213”, “gene”, “genetic”, “mutation”, “exome sequencing” were used. For Moyamoya syndrome, the following key terms were employed: “Moyamoya syndrome”, “quasi-moyamoya disease”, “Moyamoya angiopathy”, “gene”, “genetic”, and “mutation”. We

searched reference lists of relevant articles. The inclusion and exclusion criteria were as follows:

Inclusion criteria: (1) genetic studies and case reports that revealed susceptibility genes; (2) positive genes identified in studies or validated in microarray data and high-throughput sequencing; (3) data on all patients, including children, adults and different races were included. Exclusion criteria: (1) studies not related to MMD and MMS were excluded; (2) if the susceptibility genes were reported by different studies, the first article that identified the risk gene was included, and the duplicates were removed. Finally, the list of articles covering this topic was selected and the susceptibility genes were separately collected for MMD and MMS. The design of the study is illustrated in Fig. 1.

This study was approved by the Institutional Ethics Committee of The First Affiliated Hospital of Zhengzhou University.

2.2. Bioinformatics analysis

2.2.1. Gene Ontology (GO) analysis

We employed Sangerbox (version 1.1.3, http://sangerbox.com/) to obtain GO terms. Sangerbox is a comprehensive, interaction-friendly clinical bioinformatics analysis web-based tool platform [18].

MMD susceptibility genes were identified from the selected relevant articles. For GO functional enrichment analysis for MMD, we first downloaded the c5.go.bp.v7.4.symbols.gmt, c5.go.cc.v7.4.symbols.gmt and c5.go.mf.v7.4.symbols.gmt subset from the Molecular Signatures Database, which was used as the background for mapping the gene to the background set. The clusterProfiler package in R (version 3.14.3) was used for gene enrichment analysis and the results were obtained. The minimum and maximum gene sets were 5 and 5000, respectively. We chose Benjamini & Hochberg as the false discovery rate (FDR) correction method and a FDR <0.1 was used as the selection criterion.

MMS susceptibility genes were identified from the selected articles on MMS, and the same process described above was followed.

2.2.2. Kyoto Encyclopedia of Genes and Genomes (KEGG)analysis

Sangerbox was used for KEGG functional enrichment analysis. In brief, for the identified MMD susceptibility genes, the latest annotation for enriched KEGG pathways was obtained using KEGG rest API (https://www.kegg.jp/kegg/rest/keggapi.html). It was used as the background to map the gene to the background set. The clusterProfiler package in R (version 3.14.3) was used for enrichment analysis. The minimum and maximum gene sets were 5 and 5000, respectively. We chose Benjamini & Hochberg as FDR correction method and a FDR<0.1 was used as the selection threshold.

For KEGG functional enrichment of the identified MMS susceptibility genes, the same process and manual criteria were employed.

2.2.3. Analysis of protein–protein interactions (PPIs)

Since functional protein interactions usually occur between two or more components, PPI plays a major role in understanding the molecular mechanism [19]. For PPI analysis of the identified MMD susceptibility genes, the STRING (version 12.0, https://cn.string-db.org/) database [20]was used to create PPI networks with a confidence level of 0.700. In the network: a) Disconnected nodes were hidden. b) Nodes represent proteins and edges represent protein-protein associations. c) 3D bubbles were used for visualization and structures were previewed inside network bubbles. Hub genes and the most significant model were identified using the cytoHubba (version 0.1) and MCODE (version 2.0.0) plugins of Cytoscape (version 3.9.1), respectively.

The same process and criteria described above were used for PPI analysis of the identified MMS susceptibility genes.

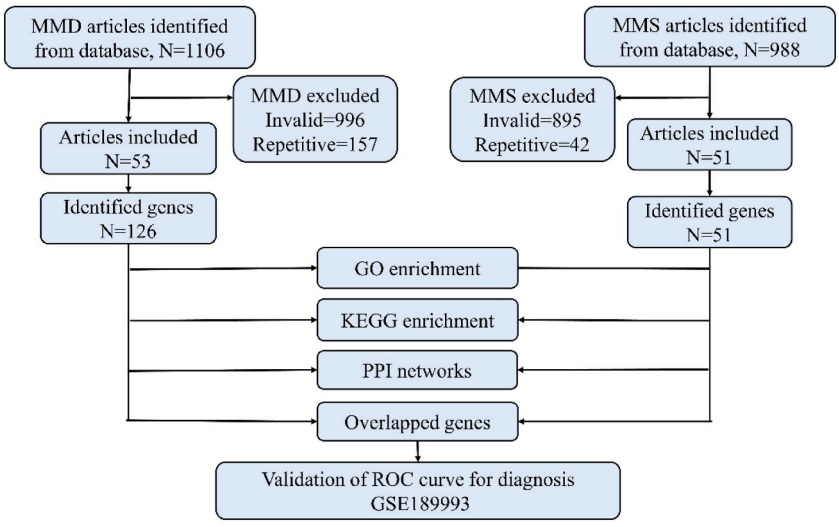

Fig. 1. The flow chart of the study design. This flow diagram includes bioinformatics analysis and validation to identify the major functional activities and risk-predictive genes between MMD and MMS.

2.3. Validation of overlapping genes and receiver operating characteristic (ROC) curve analysis

For the identified susceptibility genes in MMD and MMS, overlapping genes between MMD and MMS were screened using jvenn (http://jvenn.toulouse.inra.fr/) [21]. We selected the GSE189993 dataset considering the larger number of samples from the GEO database (https://www.ncbi.nlm.nih.gov/geo/), a public functional genomics data repository, to verify these commonly shared genes. The selected GSE189993 dataset contained data from 32 patients. Micro-samples of the middle cerebral artery (MCA) were collected during surgery from patients with MMD (n = 21) and those from control (internal carotid artery aneurysm n = 4, epilepsy n = 5). The GSE189993 dataset was downloaded and samples were divided into MMD and control groups. Information on expressions of all genes were extracted and the expression of overlapping genes were compared.

Finally, ROC curves were plotted to assess the predictive value of the validated genes in MMD, and the diagnostic ability of identified genes. The default parameters were adopted during the analysis, and no operation was manually modified. The sensitivity and specificity for diagnosis were evaluated by calculating the AUC value of the ROC curve using SPSS (Version 19.0).

2.4. Statistical analysis

Continuous and normally distributed variables are presented as mean ± standard deviation. Comparisons were conducted by Student's t-test or Mann-Whitney test using GraphPad Prism (Version 7.0). The validation using ROC curves of identified genes was plotted using SPSS software (version 19.0). Statistical significance was defined at a p-value less than 0.05.

3. Results

3.1. Common genes between MMD and MMS

According to the criteria stated above, we searched published papers, as shown in supplementary information (Supplementary1 Identified genetic studies).

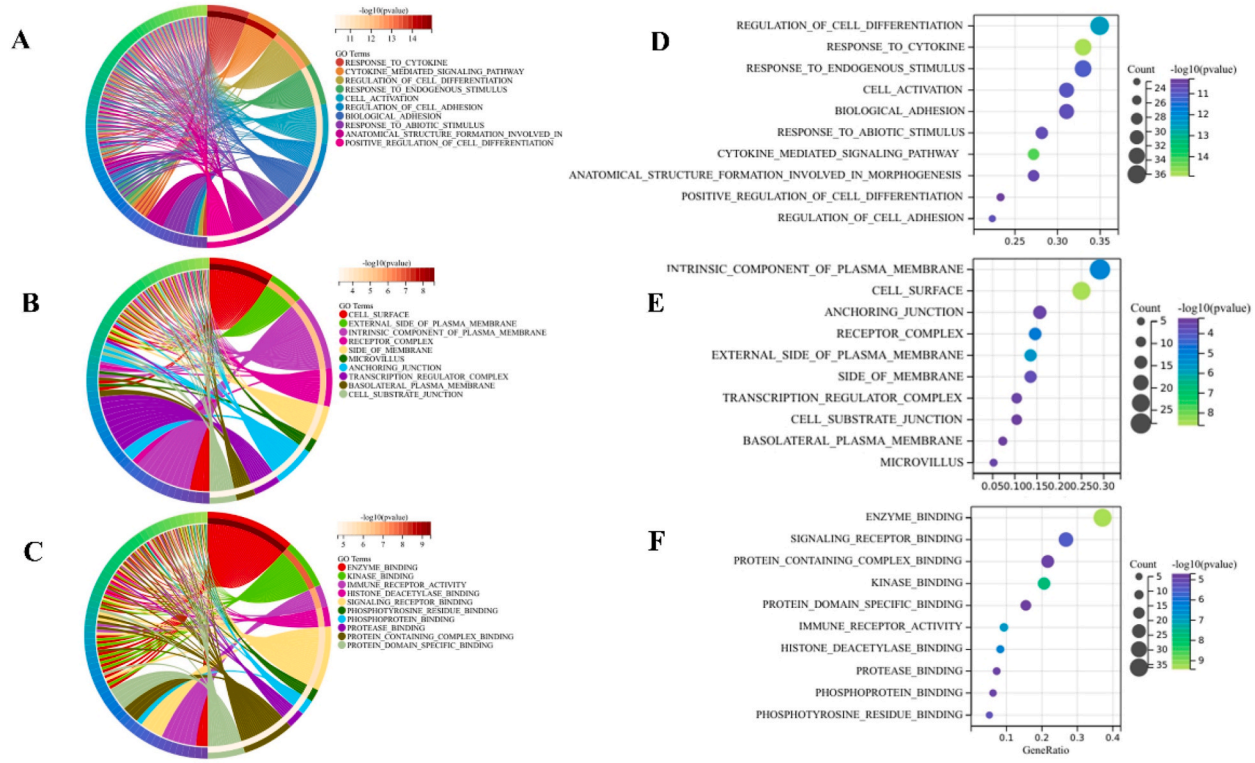

Fig. 2. Circos plot for GO functional enrichment results for MMD and bubble plot for GO functional enrichment results for MMS. GO terms related to the identified MMD susceptibility genes were enriched, and the top 10 terms were visualized using a Circos plot (A–C). Circos plot is a chart displaying complex data on functional enrichment. GO terms are colored in the right semicircle; the linked genes are colored in the left semicircle; the right inner semicircle represents -log10(p value) in red. A biological process, B cellular component, C molecular function. GO terms were enriched for the identified genes related to MMS. The top 10 terms were visualized using a bubble plot (D–F). Bubble chart is a multidimensional data display tool, which can simultaneously display multiple variables. The X-axis represents GeneRatio, the Y-axis represents enriched GO terms, and the dot represents the gene count. D biological process, E cellular component, F molecular function.

Related to MMD, 1106 articles were screened and 52 articles were enrolled, a total of 126 susceptibility genes were identified (supplementary2 Table S1). There were different types of genetic studies, including case-control studies, microarray studies, sequencing studies, case reports and bioinformatics analysis using GEO.

Related to MMS, 988 articles were screened and 51 articles were enrolled, a total of 51 susceptibility genes were identified finally. Included studies were case reports and other studies (Supplementary2. Table S1).

3.2. Results of bioinformatics analysis

3.2.1. GO enrichment between MMD and MMS

GO terms were annotated as biological processes (BP), cellular components (CC) and molecular functions (MF). The enrichment p-values for MMD and MMS were $p < 1.0e\text{-}16$ and $p = 4.48e\text{-}06$, respectively. Significant BP terms included response to cytokine, cytokine mediated signaling pathway, cell differentiation and activation (Fig. 2A). Significant CC terms included cell surface, plasma membrane and receptor complex (Fig. 2B). Significant MF terms included enzyme binding, kinase binding and immune receptor activity (Fig. 2C). The top5 most significant MF, BP and CC terms are shown in Supplementary2. Table S2.

For MMS-related susceptibility genes, GO-BP terms included heart development, locomotion, circulatory system development, tube morphogenesis and regulation of type I interferon mediated signaling pathway (Fig. 2D). Go-CC terms included motile cilium, endoplasmic reticulum lumen, dynein complex, membrane microdomain and Brcc36 isopeptidase (BRISC) complex (Fig. 2E). GO-MF terms included deoxyribonucleotide binding, insulin receptor substrate binding, DNA binding, and ATP dependent microtubule motor activity minus end directed (Fig. 2F). Top10 most significant MF, BP and CC terms are illustrated in Supplementary2. Table S3.

3.2.2. Results of KEGG enrichment analysis between MMD and MMS

Susceptibility-related genes in MMD and MMS were subjected to KEGG signaling pathway enrichment analysis. For MMD, the environmental information processing was mainly enriched in the MAPK signaling pathway and Jak-STAT signaling pathway, human disease or substances were mainly involved in pathways related to proteoglycans in cancer, chronic myeloid leukemia, graft-versus-host disease, allograft rejection and autoimmune thyroid disease. The top 20 significant KEGG enrichments for MMD are shown in Fig. 3A (Supplementary2. Table S4).

For MMS, the environmental information processing was mainly enriched in the Ras signaling pathway, Notch signaling pathway and AMPK signaling pathway, the kinds of human disease were mainly involved in Pathways in breast cancer, chronic myeloid leukemia, and endocrine resistance. One carbon pool by folate steroid hormone biosynthesis was enriched in metabolism. The top20 significant KEGG enrichments results for MMS are shown in Fig. 3B (Supplementary2. Table S5).

3.2.3. Results of PPI analysis

For the identified susceptibility genes, we constructed the PPI networks using an online tool. Abnormal PPI can cause a rare disorder. Protein subnetworks representing MMD and MMS were screened. The PPI networks of MMD included 116 nodes and 158 edges, the p-value of PPI enrichment was $p < 1.0e^{-16}$ (Fig. 4A). We used the cytoHubba plugin to identify the hub genes in the networks. *PTPN11, GRB2, CBL, CRK, ITGB3, PDGFRB, HIF1A, CCND1, MMP9,* and *CD44* were identified as the top 10 genes in MMD (Fig. 4B). We used the MCODE plugin to identify the two most significant modules in MMD. The first contained 15 genes (Fig. 4C) and

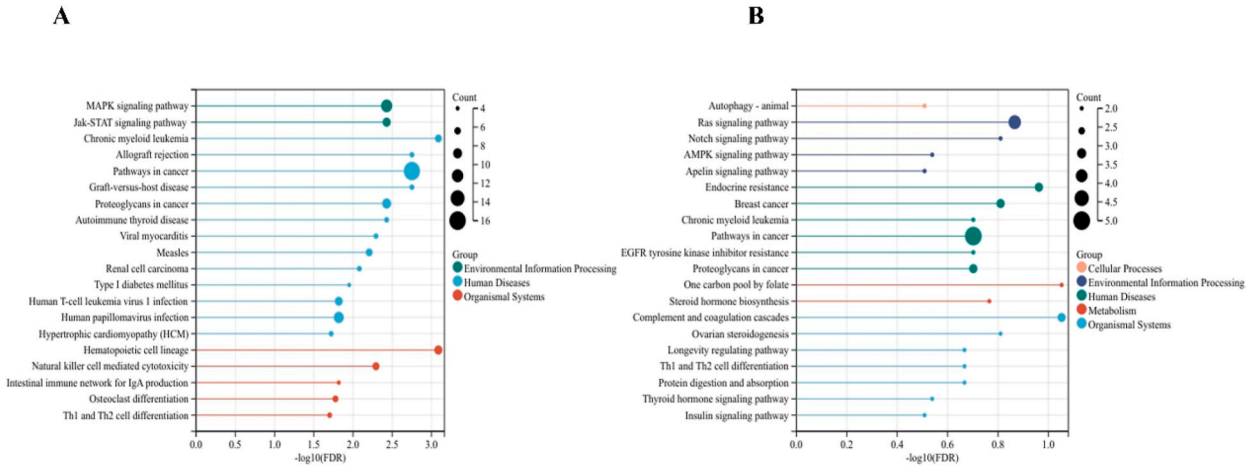

Fig. 3. Lollipop chart for KEGG functional enrichment in MMD and MMS. A KEGG signaling pathways were enriched for identified MMD susceptibility genes, in particular, and immune activities were mainly enriched. B KEGG signaling pathways were enriched for identified MMS susceptibility genes, in particular, and immune, inflammatory, and metabolic activities were enriched. The top 20 pathways were visualized using a lollipop chart, a variation of a bar chart, which compares numerical values based on the length of lines and the size of nodes. X-axis represents -log10 (FDR), the Y-axis represents enriched KEGG pathways, the dot represents gene count, and the color represents a group of KEGG pathways.

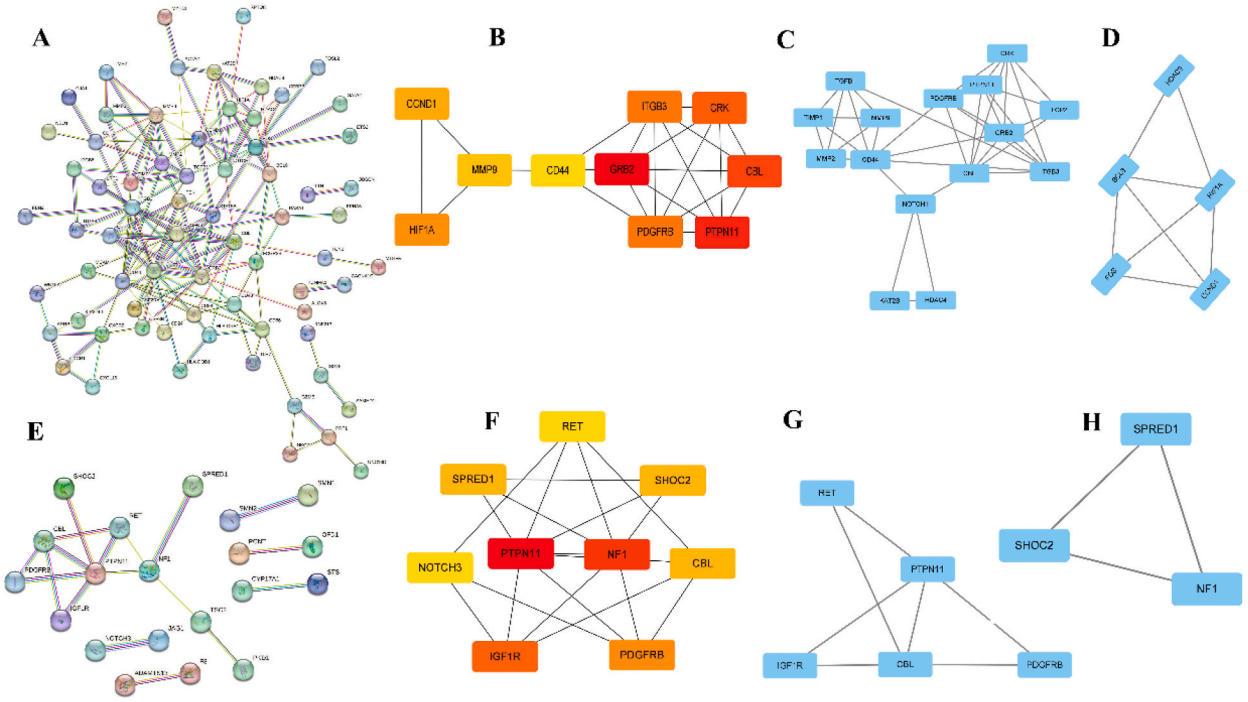

Fig. 4. Protein–protein interaction (PPI) networks, hub genes, and significant modules for MMD and MMS. PPI is an analytical approach that describes the interactions between a group of proteins. Not only can it clarify the interaction relationship between proteins but it also screens key proteins in the network. The networks were built with an interaction score of 0.700, and disconnected nodes in the network were hidden. Nodes were displayed using 3D bubbles representing proteins, protein structures were previewed inside network bubbles. Edges represent protein-protein associations. *GRB2, PTPN11, CBL, PDGFRB, CRK, ITGB3, HIF1A, CCND1, MMP9* and *CD44* were identified as hub genes in MMD. *PTPN11, NF1, IGF1R, PDGFRB, SHOC2, SPRED1, CBL, RET and NOTCH3* were identified as hub genes in MMS. A PPI network for MMD, B Hub genes identified in MMD, C The first significant model identified in MMD, D The second significant module identified in MMD. E PPI network for MMS, F Hub genes identified in MMS. G the first significant model identified in MMS, H The second significant model identified in MMS.

the second contained five genes (Fig. 4D).

The PPI network of MMS included 48 nodes and 18 edges, with a p-value PPI for enrichment of $p = 4.48e^{-06}$ (Fig. 4E). *PTPN11, NF1, IGF1R, PDGFRB, CBL, SPRED1, SHOC2, NOTCH3, RET* and *OFD1* were identified as top10 hub genes in MMS using the MCC cytoHubba algorithm (Fig. 4F). Among the identified hub genes, three were shared between MMD and MMS, namely *PTPN11, CBL, PDGFRB.* The MCODE plugin was used to identify the two most significant modules in MMS. The first contained five genes (Fig. 4G) and the second contains three genes (Fig. 4H).

3.3. Validation of overlapping genes and ROC curve analysis results

We compared the susceptibility genes related to MMD and MMS to identify the shared risk genes underlying the development of MMD and MMS. Nine shared genes were identified between 126 susceptibility genes in MMD and 51 in MMS, including *MTHFR, PTPN11, CBL, GUCY1A3, BRCC3, PDGFRB, RNF213, CNOT3,* and *SAMHD1*(Fig. 5A).

We used the microarray dataset GSE189993 from the GEO platform (Supplementary 3 Validation by the dataset GSE189993) to verify the expression of these shared susceptibility genes. The expression profiles of the nine genes were compared between the MMD and control groups, and the results showed a significant difference in *RNF213*(Fig. 5B), *PTPN11* (Fig. 5C) and *MTHFR* genes (Fig. 5D). Finally, we evaluated the diagnostic ability of the three genes for MMD using ROC curves. The AUCs of *RNF213*(Fig. 5E), *PTPN11* (Fig. 5F), and *MTHFR* (Fig. 5G) gene were 0.749, 0.874, and 0.710, respectively. For combined diagnosis with two of three genes, *PTPN11* combined with *MTHFR* demonstrated the highest diagnostic accuracy with an AUC of 0.905 and a 95 % confidence interval (CI) from 0.801 to 1.000 (Fig. 5H). For combined diagnosis using three genes, the highest diagnostic accuracy was obtained with an AUC value of 0.918 and 95 % CI from 0.824 to 1.000 (Fig. 5I).

3.4. Representative case

An 11-year-old boy was admitted to the hospital with the main complaint of intermittent fever for two weeks. The main clinical symptom of the patient was temporal headache with a peak of fever at 39.6 °C. There was no notable previous history or family history.

Hematology examination revealed the following: White blood cell count $2.68*10^{\hat{}}9$/L; red blood cell count $4.18*10^{\hat{}}9$/L;

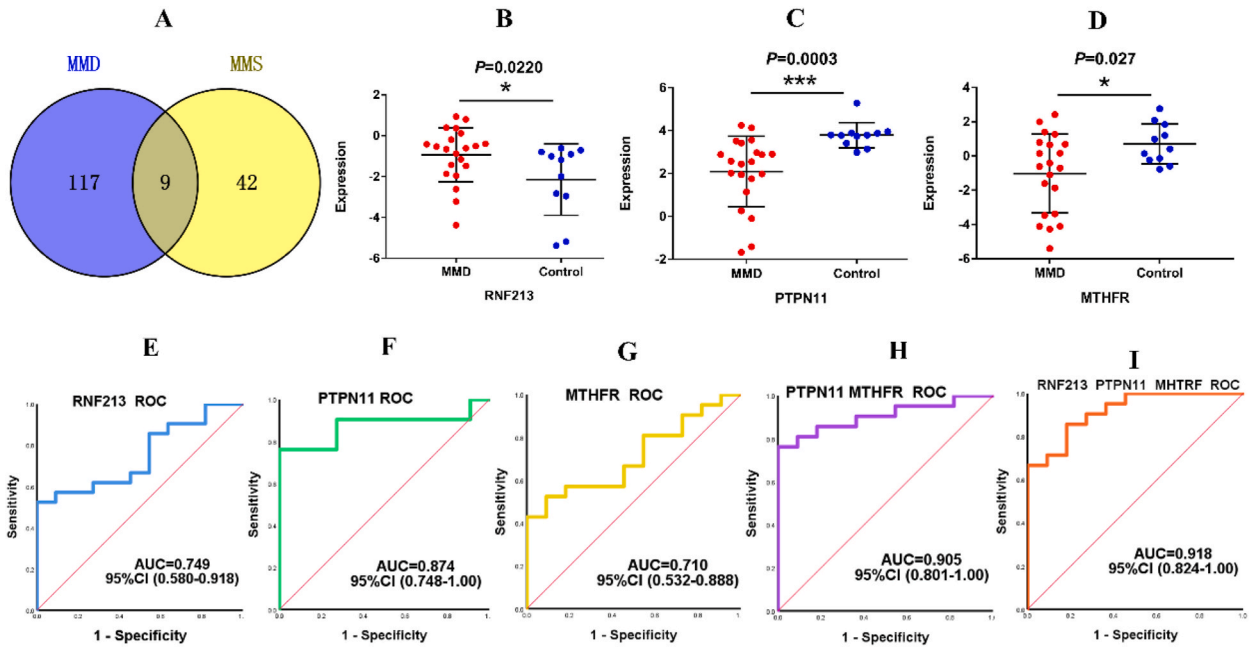

Fig. 5. Validation of common genes and diagnostic ROC curves for identified genes. A Venn plot of overlapped genes between MMD and MMS. Nine genes were identified between two groups, namely *MTHFR, PTPN11, CBL, GUCY1A3, BRCC3, PDGFRB, RNF213, CNOT3,* and *SAMHD1*. B gene expression of *RNF213*. C Gene expression of *PTPN11*. D Gene expression of *MTHFR*. E ROC curve for *RNF213*. F ROC curve for *PTPN11*. G ROC curve for *MTHFR*. H ROC curve for *PTPN11* combined with *MTHFR*. I ROC curve for the combination of *RNF213, PTPN11,* and *MTHFR*. *$p < 0.05$, **$p < 0.01$, ***$p < 0.05$ by Student's *t*-test.

hemoglobin, 114 g/L; platelet count, 259*$10^{\hat{}}9$/L; absolute neutrophil count, 1.36*$10^{\hat{}}9$/L; neutrophil percentage, 50.7 %; Lymphocyte percentage, 33.5 %; uric acid, 121 μmol/L; glutamic-pyruvic transaminase, 86U/L; glutamic oxaloacetic transaminase (GOT), 87U/L; creatine kinase, 21 U/L; lactate dehydrogenase (LDH), 543 U/L; lactate, 2.97 mmol/L; erythrocyte sedimentation rate (ESR), 79 mm/h, and C-reactive protein (CRP), 21.87 mg/L. There were no abnormalities in terms of the morphology of bone marrow cells and peripheral blood cells.

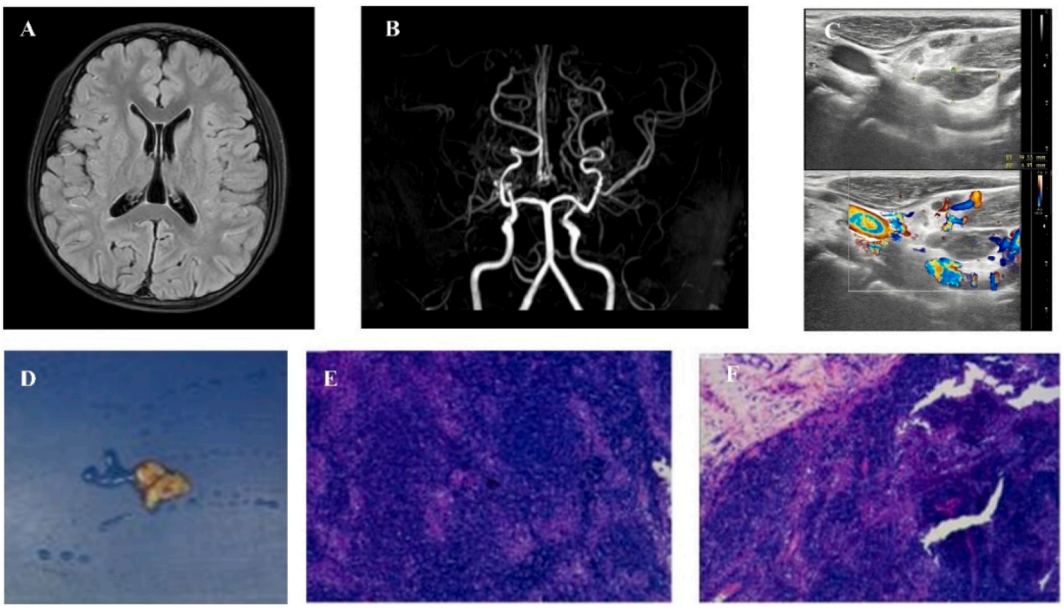

Fig. 6. Examination of our case. A Axial position of T2 FLARE magnetic resonance image. B Magnetic resonance angiography. C Ultrasound examination of cervical lymph nodes. D-F Pathology of lymphatic tissue.

Imaging examination revealed the following: magnetic resonance imaging of the head showed moyamoya vessel angiogenesis in the brain (Fig. 6A and B). The results of an ultrasound examination showed several lymph node echoes on both sides of the neck, with the larger ones located in the left IV region with a size of approximately 17.4 mm * 11 mm. CDFI showed grade I blood flow signals (Fig. 6C). However, the patient did not undergo a digital subtraction angiography examination. Cerebrospinal fluid examination showed no abnormalities.

Subsequently, the patient underwent a "left cervical lymph node resection and fascial tissue flap plasty" surgery. The pathological results showed lymphoid tissue hyperplasia with small focal necrosis. The overall view of the tissue is presented in Fig. 6D. The results of immunohistochemical analysis showed AE1/AE3 (−), CD20 (+), CD79 (+), CD3 (+), CD10(−), Bcl-2(+), Bcl-6(+), CD30(+), CD56 (+), TIA-1(+), GranzymeB(+), ALK(5A4)(−),MPO(+), CD123(+),CD68(+),S-100(+), Ki-67(70 %+), and in situ hybridization results EBER (−) status (Fig. 6E and F). After treatment, the patient's temperature remained normal, and he was discharged from the hospital. The patient was diagnosed with necrotizing lymphadenitis and moyamoya syndrome.

4. Discussion

In this study, we incorporated comprehensive and multiple types of genetic data analysis to explore the functional activities of Moyamoya disorders. The utilization of bioinformatics analysis techniques demonstrates a rigorously and skillfully implemented methodology, and the study leverages insights from multiple disciplines for a more comprehensive understanding of the disease in pathway analyses. A series of genomic and clinical MMD studies have been carried out [17,22,23], but those on MMS are limited to case reports [24,25]. A few studies focused on their pathological relationship and potential clinical impact. We first distinguished MMD and MMS based on genetic functional enrichment, bridging gaps in the field. It makes a noteworthy contribution to comprehending both illnesses and offers useful insights into pathological research. Our results revealed the close association of MMD with immune activity, MMS showed a close relationship with inflammatory response, metabolism disorders, and other environmental factors with the susceptible genetic background. For KEGG functional enrichment, immunological activities were involved in both MMD and MMS, including autoimmune thyroid disease, thyroid hormone signaling pathway, type I diabetes mellitus, Th1 and Th2 cell differentiation, and allograft rejection. A growing number of molecular and clinical reports have described MMD emerging as immune-related angiopathy [26]. Immune infiltration analysis demonstrated a significantly different proportion of eosinophils, neutrophils, monocytes, Th2 cells and natural killer cells in MMD [27]. Our results were consistent with those of previous studies. The human disease pathway in cancers and chronic myeloid leukemia was enriched in both MMD and MMS in our study. Though the cerebral vascular disease was not cancer, moyamoya disorders associated with brain glioblastoma [28] and other cancers have been investigated. Studies based on bioinformatics analysis have demonstrated shared molecular biomarkers that link MMD and glioblastoma [29]. These studies suggest that the Moyamoya vessels may share common complex and potential molecular mechanisms in the pathogenesis of these diseases, mainly through new vessel formation during tumor growth [30]. Notably, the signaling pathways enriched in MMD mainly regulate the immune and cell activities, while the pathways enriched in MMS are closely related to inflammation and metabolism. Interestingly, signaling pathways showed greater enrichment in MMS compared to MMD in this study, suggesting heterogeneous and complex activities underlying the development of MMS. Considering the similarities and differences between MMD and MMS, our results reveal new clues for disease prevention, clinical management, and treatment strategies, especially targeting the pathological mechanisms during disease progression.

Furthermore, we identified nine common genes shared between MMD and MMS. The expressions of *RNF213, PTPN11,* and *MTHFR* showed significant differences in the validation dataset. Validation provides critical evidence for the reliability and potential applicability of these results. As the first identified risk gene for MMD [17], multiple studies have confirmed the strong association between *RNF213* and MMD, and elucidated the function of *RNF213* in the East Asian population [31]. It is a multifunctional protein involved in several key cellular processes, including LD stability [32], WNT [33] NF-κB signaling and inflammation [34]. Changes in di-saturated glycerolipids are central to lipotoxicity, and the depletion of *RNF213* protects cells from lipotoxicity [35]. Thus, *RNF213* variants, such as p.R4810K, should be considered susceptibility rather than causative variants for MMD. However, the roles of *PTPN11* and *MTHFR* in Moyamoya have not been fully understood. *PTPN11* encodes the protein tyrosine phosphatase SHP-2, which regulates the RAS signaling pathway. *PTPN11* mutations are commonly associated with Noonan syndrome [36] and MMS occurs with Noonan syndrome. *MTHFR* is crucial in folate metabolism, the pathway involved in the functional activities for cell metabolism in RNA, DNA, and protein methylation [37], for example, the remethylation of homocysteine to methionine and one-carbon cycle [38]. Both *RNF213* and *MTHFR* are significant in the metabolism process. Metabolism pathways were enriched in MMS, including one carbon pool by folate and steroid hormone biosynthesis. These identified and validated genes may have important implications for the diagnosis, treatment, and management of MMD and MMS.

Recently, a second hit theory has been hypothesized as the pathological mechanism underlying MMD. There are strongly suspected genetic contributions in the published research, and environmental factors play an important role in triggering the MMD. Several studies suggest radiation, autoimmune conditions, bacterial infections and viral infections, including varicella zoster virus (VZV), cytomegalovirus (CMV) and Epstein-Barr virus (EBV) infections as potential environmental triggers; however, these have not been detected in most of the affected populations [39]. A majority of growth factors, enzymes, and peptides increase in MMD, including basic fibroblast growth factor, hypoxia-inducing factor, hepatocyte growth factor, transforming growth factor, vascular endothelial growth factor, intracellular adhesion molecules and matrix metalloproteinases. However, it's difficult to determine whether these changes are primary or secondary to chronic ischemia. Combining the literature and our results, Moyamoya vasculopathy seems more likely to be a polygenic and multifactorial disease entity.

Some limitations in the study should be acknowledged. First, the study relied on published literature, especially on certain ethnic

groups at higher risk for MMD. Thus, there may be a publication bias toward positive findings. Second, there were limitations inherent in bioinformatics analysis and the use of databases for GO, KEGG enrichment, and PPI analyses. Updates to these databases or differences in algorithms could potentially affect the results. Third, the approaches used might simplify the complex interactions and regulatory mechanisms involved in MMD and MMS pathogenesis, and may potentially overlook epistatic effects or gene-environment interactions. Finally, MMD is a complex disease involving multiple factors, such as race, age, sex, genetic and environmental factors along with comorbidities. Overlooking these factors in the research could affect the observed associations between genetic markers and MMD/MMS.

5. Conclusions

In summary, we clarified the functional activities and overlapping genes to distinguish MMD from MMS. Functional enrichment of MMD was mainly involved in immune activities while MMS was involved in different types of functional activities, such as inflammatory activity and metabolic activity. *RNF213, PTPN11* and *MTHFR* were shared between MMD and MMS and validated in an independent dataset. Differential functional activities provided a deeper understanding of the Moyamoya disorders, while the shared functional activities may suggest major pathological mechanisms. The findings can importantly guide clinical practice and may have wider ramifications in pathological research and clinical management. These findings provided novel avenues for future pathological mechanism research and potential impact on diagnosis and therapy. In the future, more in-depth studies of immune, inflammatory, and metabolic activities should be focused on and carried out.

Funding statement

This research received no external funding.

Data availability statement

Validation data of our study were openly available from the GEO (GSE189993) database (https://www.ncbi.nlm.nih.gov/geo/query/acc.cgi). The data underlying this article are publicly available alongside the article upon publication.

CRediT authorship contribution statement

Lei Cao: Writing – original draft, Methodology, Data curation, Conceptualization. **Wenzhi Yang:** Methodology, Formal analysis, Data curation. **Xiaozong Duan:** Methodology, Formal analysis, Data curation. **Yipu Shao:** Visualization, Data curation. **Zhizhong Zhang:** Validation, Data curation. **Chenchao Wang:** Visualization, Data curation. **Kaiwen Sun:** Visualization, Data curation. **Manxia Zhang:** Visualization, Resources. **Hongwei Li:** Writing – review & editing, Supervision, Conceptualization. **Kouji H. Harada:** Writing – review & editing, Supervision, Conceptualization. **Bo Yang:** Writing – review & editing, Supervision, Conceptualization.

Declaration of competing interest

The authors declare that they have no known competing financial interests or personal relationships that could have appeared to influence the work reported in this paper.

Acknowledgments

We acknowledge the GEO database for providing their platforms and contributors for uploading their meaningful datasets.

Appendix A. Supplementary data

Supplementary data to this article can be found online at https://doi.org/10.1016/j.heliyon.2024.e34600.

References

[1] J. Suzuki, A. Takaku, Cerebrovascular "moyamoya" disease. Disease showing abnormal net-like vessels in base of brain, Arch. Neurol. 20 (3) (1969) 288–299.
[2] M. Fukui, Guidelines for the diagnosis and treatment of spontaneous occlusion of the circle of willis ('moyamoya' disease). Research committee on spontaneous occlusion of the circle of willis (moyamoya disease) of the ministry of health and welfare, Japan, Clin. Neurol. Neurosurg. 99 (Suppl 2) (1997) S238–S240.
[3] E.R. Smith, R.M. Scott, Progression of disease in unilateral moyamoya syndrome, Neurosurg. Focus 24 (2) (2008) E17.
[4] R.J. Doherty, et al., Moyamoya disease and moyamoya syndrome in Ireland: patient demographics, mode of presentation and outcomes of EC-IC bypass surgery, Ir. J. Med. Sci. 190 (1) (2021) 335–344.
[5] S. Currie, et al., Childhood moyamoya disease and moyamoya syndrome: a pictorial review, Pediatr. Neurol. 44 (6) (2011) 401–413.
[6] L. Thines, et al., Surgical management of Moyamoya disease and syndrome: current concepts and personal experience, Rev. Neurol. (Paris) 171 (1) (2015) 31–44.
[7] P. Fiaschi, et al., Limits and pitfalls of indirect revascularization in moyamoya disease and syndrome, Neurosurg. Rev. 44 (4) (2021) 1877–1887.

[8] R.M. Scott, E.R. Smith, Moyamoya disease and moyamoya syndrome, N. Engl. J. Med. 360 (12) (2009) 1226–1237.
[9] R.M. Scott, et al., Long-term outcome in children with moyamoya syndrome after cranial revascularization by pial synangiosis, J. Neurosurg. 100 (2 Suppl Pediatrics) (2004) 142–149.
[10] L. Grangeon, et al., Clinical and molecular features of 5 European multigenerational families with moyamoya angiopathy, Stroke 50 (4) (2019) 789–796.
[11] P. Hever, A. Alamri, C. Tolias, Moyamoya angiopathy - is there a Western phenotype? Br. J. Neurosurg. 29 (6) (2015) 765–771.
[12] H. Ikeda, et al., Mapping of a familial moyamoya disease gene to chromosome 3p24.2-p26, Am. J. Hum. Genet. 64 (2) (1999) 533–537.
[13] T.K. Inoue, et al., Linkage analysis of moyamoya disease on chromosome 6, J. Child Neurol. 15 (3) (2000) 179–182.
[14] K. Sakurai, et al., A novel susceptibility locus for moyamoya disease on chromosome 8q23, J. Hum. Genet. 49 (5) (2004) 278–281.
[15] T. Yamauchi, et al., Linkage of familial moyamoya disease (spontaneous occlusion of the circle of Willis) to chromosome 17q25, Stroke 31 (4) (2000) 930–935.
[16] W. Liu, et al., Identification of RNF213 as a susceptibility gene for moyamoya disease and its possible role in vascular development, PLoS One 6 (7) (2011) e22542.
[17] F. Kamada, et al., A genome-wide association study identifies RNF213 as the first Moyamoya disease gene, J. Hum. Genet. 56 (1) (2011) 34–40.
[18] W. Shen, et al., Sangerbox: a comprehensive, interaction-friendly clinical bioinformatics analysis platform, iMeta 1 (3) (2022) e36.
[19] J. De Las Rivas, C. Fontanillo, Protein-protein interactions essentials: key concepts to building and analyzing interactome networks, PLoS Comput. Biol. 6 (6) (2010) e1000807.
[20] D. Szklarczyk, et al., STRING v10: protein-protein interaction networks, integrated over the tree of life, Nucleic Acids Res. 43 (Database issue) (2015) D447–D452.
[21] P. Bardou, et al., jvenn: an interactive Venn diagram viewer, BMC Bioinf. 15 (1) (2014) 293.
[22] L. Duan, et al., Novel susceptibility loci for moyamoya disease revealed by a genome-wide association study, Stroke 49 (1) (2018) 11–18.
[23] J. Wan, et al., Association of HLA-DQA2 and HLA-B with moyamoya disease in the Chinese han population, Neurol Genet 7 (3) (2021) e592.
[24] E. Tzeravini, et al., Severe hemophilia A and moyamoya syndrome in a 19-year-old boy caused by Xq28 microdeletion, Case Rep. Neurol. 14 (2) (2022) 261–267.
[25] L. Pabst, et al., Moyamoya syndrome in a child with Legius syndrome: introducing a cerebral vasculopathy to the SPRED1 phenotype? Am. J. Med. Genet. 185 (1) (2021) 223–227.
[26] C. Asselman, et al., Moyamoya disease emerging as an immune-related angiopathy, Trends Mol. Med. 28 (11) (2022) 939–950.
[27] F. Jin, C. Duan, Identification of immune-infiltrated hub genes as potential biomarkers of Moyamoya disease by bioinformatics analysis, Orphanet J. Rare Dis. 17 (1) (2022) 80.
[28] S. Kitano, et al., Moyamoya disease associated with a brain stem glioma, Childs Nerv Syst 16 (4) (2000) 251–255.
[29] M.K. Islam, et al., Bioinformatics strategies to identify shared molecular biomarkers that link ischemic stroke and moyamoya disease with glioblastoma, Pharmaceutics 14 (8) (2022).
[30] M. Lim, S. Cheshier, G.K. Steinberg, New vessel formation in the central nervous system during tumor growth, vascular malformations, and Moyamoya, Curr. Neurovascular Res. 3 (3) (2006) 237–245.
[31] R. Mertens, et al., The genetic basis of moyamoya disease, Transl Stroke Res 13 (1) (2022) 25–45.
[32] M. Sugihara, et al., The AAA+ ATPase/ubiquitin ligase mysterin stabilizes cytoplasmic lipid droplets, J. Cell Biol. 218 (3) (2019) 949–960.
[33] M. Takeda, et al., Moyamoya disease patient mutations in the RING domain of RNF213 reduce its ubiquitin ligase activity and enhance NFκB activation and apoptosis in an AAA+ domain-dependent manner, Biochem. Biophys. Res. Commun. 525 (3) (2020) 668–674.
[34] V. Roy, et al., Moyamoya disease susceptibility gene RNF213 regulates endothelial barrier function, Stroke 53 (4) (2022) 1263–1275.
[35] M. Piccolis, et al., Probing the global cellular responses to lipotoxicity caused by saturated fatty acids, Mol. Cell. 74 (1) (2019) 32–44.e8.
[36] M. Tartaglia, et al., PTPN11 mutations in Noonan syndrome: molecular spectrum, genotype-phenotype correlation, and phenotypic heterogeneity, Am. J. Hum. Genet. 70 (6) (2002) 1555–1563.
[37] S.C. Liew, E.D. Gupta, Methylenetetrahydrofolate reductase (MTHFR) C677T polymorphism: epidemiology, metabolism and the associated diseases, Eur. J. Med. Genet. 58 (1) (2015) 1–10.
[38] S. Raghubeer, T.E. Matsha, Methylenetetrahydrofolate (MTHFR), the one-carbon cycle, and cardiovascular risks, Nutrients 13 (12) (2021).
[39] Y. Nakamura, et al., Lack of association between seropositivity of vasculopathy-related viruses and moyamoya disease, J. Stroke Cerebrovasc. Dis. 31 (7) (2022) 106509.